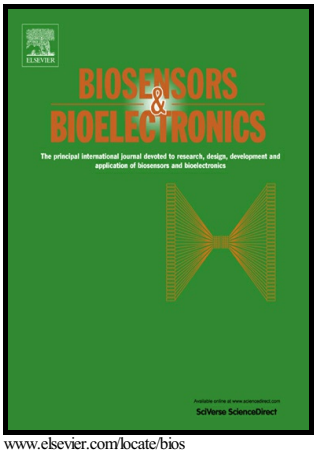

www.elsevier.com/locate/bios

A highly sensitive self assembled monolayer modified copper doped zinc oxide nanofiber interface for detection of plasmodium falciparum histidine-rich protein-2: Targeted towards rapid, early diagnosis of malaria

K Brince Paul, Sanni Kumar, Suryasnata Tripathy, Siva Rama Krishna Vanjari, Vikrant Singh, Shiv Govind Singh

PII: S0956-5663(16)30035-5
DOI: http://dx.doi.org/10.1016/j.bios.2016.01.036
Reference: BIOS8376

To appear in: *Biosensors and Bioelectronic*

Received date: 19 November 2015
Revised date: 10 January 2016
Accepted date: 12 January 2016

Cite this article as: K Brince Paul, Sanni Kumar, Suryasnata Tripathy, Siva Ram Krishna Vanjari, Vikrant Singh and Shiv Govind Singh, A highly sensitive self assembled monolayer modified copper doped zinc oxide nanofiber interface fo detection of plasmodium falciparum histidine-rich protein-2: Targeted towards rapid, early diagnosis of malaria, *Biosensors and Bioelectronic* http://dx.doi.org/10.1016/j.bios.2016.01.036

A Highly Sensitive Self Assembled Monolayer Modified Copper doped Zinc Oxide Nanofiber Interface for detection of Plasmodium falciparum Histidine-Rich Protein-2: Targeted towards rapid, early diagnosis of Malaria

Brince Paul K[a] , Sanni Kumar[a] , Suryasnata Tripathy[a], Siva Rama Krishna Vanjari[a] , Vikrant Singh[b] , Shiv Govind Singh[a,*]

[a]Department of Electrical Engineering, Indian Institute of Technology, Hyderabad, India

[b]School of Medicine, University of California Davis, USA.

Abstract

Rapid, ultrasensitive diagnostic/triaging kits for early detection of malarial parasites are critical for prevention of malarial epidemic, especially in developing and tropical countries. Unlike traditional microscopic diagnosis, these kits rely on the detection of antigens specific to malarial parasites. One such antigen which is routinely used in these diagnostic kits is Histidine-rich protein-2 ; a protein synthesized and released into the blood stream by the parasite Plasmodium falciparum. In this paper, we demonstrate an ultrasensitive nanobiosensor detection platform for Histidine-rich protein-2 having a limit of detection of attogram/ml. This nanobiosensor platform comprises of Mercaptopropylphosphonic acid functionalized copper doped zinc oxide nanofibers synthesized by electrospinning technique. Ultrasensitivity of attogram/ml can be attributed to the complimentary effects of Mercaptopropylphosphonic acid and copper doping in zinc oxide. Mercaptopropylphosphonic acid enhances the functional groups required for immobilizing antibody. Copper doping in zinc oxide not only increases the conductivity of the nanofibers but also pre-concentrates the target analyte onto the Mercaptopropylphosphonic acid treated nanofiber surface due to inherent electric field generated at the copper/zinc oxide heterojunction interface. The impedimetric detection response of copper-doped Zinc oxide nanofiber modified electrode shows excellent sensitivity (28.5 KΩ/(gm/ml)/cm^2) in the detection ranges of 10ag/ml-10µg/ml, and a detection limit of 6 attogram/ml. In addition, the proposed biosensor is highly selective to targeted HRP2 protein with a relative standard deviation of 1.9% in the presence of various interference of nonspecific molecules. To the best of our knowledge, this biosensor shows the lowest detection limit of malarial parasites reported in the literature spanning different nanomaterials and different detection mechanisms. Since the nanobiosensor platform is based on immunoassay technique, with a little modification, it can be extended for developing point-of-care diagnostic devices for several biomarkers of importance.

Keywords: Nanobiosensor, Mercaptopropylphosphonic acid, Attogram, Ultrasensitivity, Histidine-rich protein-2, Malaria.

1. Introduction

Malaria epidemic is considered as one of the biggest public health challenges, especially in developing countries. According to 2014 World health organization (WHO) reports, about 198 million people are at a high risk of malaria and it kills about 584,000 people across the globe annually. It is an infectious disease caused by parasitic Plasmodium protozoans, the pre-dominant one being Plasmodium falciparum (P. falciparum) species, which is regarded as the most lethal form of malaria (Snow et al., 2005). The gold standard that is routinely followed for diagnosing malaria is the traditional microscopic examination (Warhurst and Williams.,1996; Chotivanich et al.,2006; Erdman and Emerson.,2008). Through this routine examination a skilled microscopist can differentiate plasmodium falciparum, however, the reliability of detecting low level parasitaemia is not guaranteed. In order to overcome this, several techniques such as flow cytometry (Wongchotigul et al.,2004; Shapiro and Mandy., 2007), Polymerase Chain Reaction (PCR) based detection (Johnston et al.,2006), automated blood cell analyzers (Campuzano-Zuluaga et al., 2010), Lamp technique (Poon et al., 2006a), Mass spectrophotometry (Demirev., 2004), microarrays (Yatsushiro et al., 2010; Doolan et al.,2008), Enzme Linked Immunoabsorbent Assay ELISA (Kifude et al., 2008), molecular diagnostic methods (Fontecha et al.,2012; Poon et al.,2006b), etc., were developed. These techniques, though reliable are time consuming, costly and need skilled man power.

Rapid qualitative diagnostics kits have been developed for detection of plasmodium (Moody .,2002; Rakotonirina et al.,2008). These are lateral flow sandwich immunoassay devices wherein monoclonal antibody of plasmodium immobilized onto the detection pad, is used to bind the target antigen. The binding event is recognized calorimetrically with the help of gold nanoparticle immobilized polyclonal antibodies. These tests are qualitative and cannot detect parasitemia below 100 parasites /µl of blood. In order to prevent malaria becoming an epidemic, the need of the hour is to develop a low cost triaging device which can push the detection limits to as low as possible. Researchers have explored electrochemical method of malaria detection based on carbon nanotubes (Sharma et al.,2008) and Magneto immunoassay-based (de Souza Castilho et al.,2011) which could achieve a detection limit of few ng/ml. In

this endeavor, we propose a novel metal oxide semiconductor based nanobiosensor platform to push the detection limits all the way to few attogram/ml. This methodology is miniaturizable and can act as a tool for early stage detection of malaria which would potentially enable prevention of the epidemic.

The advent of nanoscience and nanotechnology has led to the development of various nanomaterials which explore the inherent advantages of nanoregime.The multifunctional nanomaterials have found several interesting application for sensitive and selective detection of ions (Bojdi et al.,2015; Bojdi et al.,2014a; Bojdi et al.,2014b) and biological samples (Bojdi et al., 2015;Hosseini et al.,2014). Recently, Gikunoo et al., (Gikunoo et al.,2014) reported direct detection of Plasmodium falciparum histidine rich protein-2 (PfHRP-2) antigen as low as 0.01 ng/ml by using carbon nanofibers grown on glass microbaloons. However, the synthesis procedure involved is complex. An alternative material which is easily synthesizable and at the same time possesses the capabilities of detecting minutest quantities of target species is worth exploring. Metal oxide based nanostructure materials have garnered quite a bit of attention in various domains in general and point of care diagnostics in particular. Their wide range of conductivity, high biological activity, and enhanced sensitivity makes them suitable for several biosensing applications (Solanki et al.,2011). Among the metal oxides Zinc Oxide has received wide attention owing to its unique properties such as wide band gap (3.37eV), free-exciton binding energy (60 meV), good electrochemical properties, and high isoelectric point (IEP) of about 9.5 (Ahmad et al.,2010a; Ahmad et al .,2014). The high IEP property of ZnO is an added advantage for biosensor development as it can attract and bind the target analyte molecules electrostatically. Furthermore, ZnO plays important role in electrochemical biosensors due to its higher diffusion coefficient and electron mobility compared to other metal oxide nanofibers or nano structures (Mali et al. ,2013). The non-toxicity, high thermal and chemical stability properties make ZnO an ideal candidate for developing implantable biosensors (Ahmad et al., 2010b). Recently several highly sensitive electrochemical biosensors based on ZnO nanomaterial have been reported for detection of cancer biomarkers (Hong et al.,2011;Vasudev et al.,2013; Ali et al.,2015), DNA detection(Das et al.,2010; Tak et al.,2014), uric acid detection (Tak et al.,2014) and detection of glucose (Zhao et al. 2007; Dai et al. 2009; Wei et al. 2010).

One of the major drawbacks of ZnO that needs attention while developing biosensors is the inherent high resistivity due to its high band gap. A potential solution for this is to dope ZnO nanostructures with suitable dopant which can reduce the band gap thereby increasing the conductivity and sensitivity simultaneously (Tak et al. ,2013). Reasonable doping of Cu induces an acceptor band which reduces the effective band gap and enhances the conductivity (Singhal et al.,2012). Ultra-fast charge transport between ZnO and Cu has been recently reported (Chow et al. ,2013). There have been few studies on sensing properties of Cu doped ZnO (Gong et al.,2006;Sonawane et al.,2008). A few reports are available in literature on Cu-ZnO hybrid nanostructures for biosensing application including cholesterol detection (Batra et al.,2015), which exhibits high sensitivity about 760 mA mM^{-1} cm^{-2} and ultra-sensitive glucose sensor with sensitivity of about 760 µA mM^{-1} cm^{-2}. The synthesis methodologies adapted in these works are complex. Alternatively, in this work, we have explored electrospinning technique for synthesizing Cu doped Zinc Oxide nanofibers. Electrospinning is a simple, robust, well explored low cost method of producing nanofibers. ZnO nanofibers can easily be synthesized and doped using electrospinning (Batra et al. ,2015). The surface modification of ZnO synthesized using electrospinning is a relatively straightforward process. Antibodies can easily be physisorbed onto the surface electrostatically. Alternatively, Self-Assembled Monolayers can easily be formed on the surface of ZnO which in turn can be used to covalently immobilize antibodies. Combining Cu doping and surface modification methodology could potentially lead to the minimum possible detection limit with high sensitivity. In this paper, we demonstrate an ultra-sensitive malaria electrochemical immunoassay biosensor platform utilizing MPA modified Cu doped ZnO electrospun nanofibers. Histidine-rich protein-2(HRP2) which is routinely used in rapid diagnostic kits is chosen as the target molecule. It is a protein synthesized and released into the blood stream by the parasite Plasmodium falciparum, the most lethal and most prominent variant of malaria. Cu doping in ZnO enhances the conductivity. MPA modification aids in chemically immobilization of Anti-HRP2. Electrochemical Impedance Spectroscopy technique is used as transduction mechanism as it is a very efficient technique for analyzing adsorption kinetics. Supplementary Scheme S1 shows the schematic of entire process for developing the proposed nanobiosensor platform. The platform showed excellent electrochemical characteristics with ultra-sensitivity and good stability with a detection limit of attogram/ml.

2. Materials and Methods

2.1. Materials

Polyarcylonitile (PAN, MW=1,50,000), N, N dimethyl-formamide (DMF), Zinc acetate (Zn (CH3COO)2.2H2O, 99%),Copper(II) nitrate ($Cu(NO3)_2$.3H2O, 99%), Bovine serum albumin (BSA), Phosphate buffer saline (PBS (PH 7.4)), N-hydroxysuccinimide (NHS) and N-ethyl-N0-(3-dimethylaminopropyl carbodiimide) (EDC), were obtained from SigmaAldrich ,USA. Malaria Histidine Rich Protein II (HRP2) and monoclonal malaria Histidine-Rich Protein II antibody (Anti HRP2), were purchased from Fitzgerald, USA. The Deionized distilled water (Resistivity18.2MΩ − cm) from Millipore water purification system has been used for all experiments. All the other chemical reagents were of analytical grade and were used with any further purification.

2.2. Apparatus

The morphology of synthesized Cu-doped ZnO nanofibers was observed using Field emission scanning electron microscopy (FE-SEM; Supra 400VP,Zeiss, Germany) and elemental composition of nanofibers was carried out using Energy-dispersive X-ray spectroscopy(EDX; Oxford Instruments). The crystal phase information of synthesized Cu-doped ZnO nanofiber was analysed using X-ray diffraction measurements (XRD; XPert Pro, PAN Analytical, Netherlands,X-ray system with Cu Kα radiation and λ = 1.54 A◦). Optical properties of Cu doped ZnO nanofibers were investigated with the help of UV-visible analysis (UV-Vis;Varian Cary 50Bio, UV-vis spectrophotometer). FT-IR studies (FT-IR; Perkin-Elmer, Model 2000) were performed to reaffirm the binding of Self assembled monolayer onto ZnO nanofibers. All electrochemical measurements were performed using an electrochemical analyzer CHI660E (CH Instruments, TX, USA) on a electrochemical system comprising 3mm glassy carbon electrode (GCE) modified with nanofibers as working electrode, platinum wire as auxiliary electrode, saturated calomel electrode (SCE) as reference electrode and a 0.01M phosphate buffer saline (PBS pH7.4) containing 5 mM of probe redox couple potassium ferricyanide and ferrocyanide [F e(CN)6] 3−/4−) 142].

2.3. Synthesis of Cu doped ZnO nano-fibers (CZnONF)

The first step in synthesis of electrospun Cu doped ZnO nanofibers is the preparation of homogenous precursor solution. Known weight percentages of Zinc acetate and different weight percentages of Copper nitrate were added to N,N-dimethylformamide (DMF) and the mixture was subjected to rigorous stirred for 2 hours at 60 °C. Immediately after that, desired amount of PAN was added to the mixture and the mixture was stirred for three more hours to obtain the desired homogeneous precursor solution. The solution was then loaded into 5ml syringe with 26 gauge metallic needle for electrospinning. An electric field 2 kV/cm was applied in between needle tip and silicon substrate ground and feeding rate was 40 µl/min. After 3 hours of electrospinning, thick free standing mat of non-woven fibers was extracted from silicon substrate. Calcination was carried out 550° C for 2 hours to obtain undoped or Cu-doped ZnO nanofibers after decomposition of PAN (Zhang et al. ,2009).The procedure for synthesizing pure ZnO nanofibers is exactly same but for the absence of Copper nitrate precursor.

2.4. Preparation of CZnONF/GCE electrode

The surface immobilization protocol starts with drop casting of CZnONF dispersion onto a clean polished GCE. GCE was polished thoroughly with 0.05 µm alumina slurry, followed by rinsing with DI water and air drying. The casting dispersion was prepared by adding 0.5 mg of free standing CZnOF nanofiber mat in 1ml of DMF followed by ultrasonication for 1 hour. 6 µl of the dispersion was drop cast onto the polished GCE and was allowed to dry under controlled room temperature ambience. Prior to surface immobilization of antibody, the modified electrode was washed thoroughly with deionized water to remove loosely bound or unbound nanofiber suspension. For comparison pure ZnONF modified GCE was also prepared following a similar protocol.

2.5. Mercaptopropionic acid (MPA)treatment

Chemisorption is the preferred mode of asorption of antibodies as it binds antibodies effectively onto the surface. Antibodies, being protein molecules, have amine and carboxylic groups which can be linked to any other surface having functional groups using well known linking protocols. In order to create these functional groups, MPA treatment was carried out. MPA treatment was

performed by immersing CZnONF modified GCE electrode in a 10mM Mercaptopropionic acid prepared in ethanol for 15 hours at room temperature. Subsequently, modified electrode was rinsed with deionized water and dried in air before the antibody immobilization. MPA inherently has carboxylic (-COOH) group and forms a nice self-assembled monolayer on ZnO via interaction of hydrosulphide group (HS−) with Zn^{2+} (Simˇs´ıkov´a et al.,2013). Thus MPA treatment results in abundant carboxylic groups on CZnONF.

2.6. Anti-HRP2 Immobilization

Antibodies were chemically attached to MPA functionalized Cu-doped ZnO nanofibers [fCZnONF] using well established EDC-NHS crosslinking chemistry. The carboxylic groups on GCE/fCZnONF were activated with the help of EDC and NHS. Onto this electrode, 6 µl of Anti-PfHRP2 (200 µg/ml) was drop casted and the electrode was stored at 4°C overnight. Antibodies get immobilized covalently onto fCZnONF via the amide bonds formed between amine groups of antibodies and activated carboxylic groups of fCZnONF. After chemisorption, GCE/fCZnONF/Anti-PfHRP2 was thoroughly washed with DI water (PH7.0) to remove unbound antibodies. This was followed by the treatment with BSA solution (1%wt) to block nonspecific sites. The electrode was kept at 4°C, when not in use.

3. Results and Discussions

3.1 Evaluation of nanofiber characteristics

The FESEM images of ZnO nanofibers and Cu doped ZnO (CZnONF) nanofibers pre and post calcination is shown Fig.1A. Before calcination, both undoped and doped nanofibers are smooth and uniform in nature owing to the presence of PAN. The diameter of undoped fibers and doped fibers were in the range of 300-400 nm (Fig. 1A (a)) and 700-800 nm (Fig. 1(c)) respectively, for the same electrospinning parameters. After calcination, formation of crystalline ZnO and Cu doped ZnO fibers were observed. The diameters of the fibers shrunk to 100-150 nm (Fig. 1A (b)) in the case of ZnO nanfibers and 150-200 nm (Fig. 1A (d)) in the case of Cu doped ZnO fibers. The increase in diameter latter case can be attributed to the doping of Cu in ZnO. To prove the presence of Cu in the doped fibers, EDX analysis (Fig. 1B) was carried out on undoped and doped fibers post calcination. The distinct presence of elemental Cu in the doped fibers is an affirmation that Cu is doped in ZnO.

The preferred position for Figure 1

Fig. 2 shows the XRD data for both CZnONF and pure ZnO nanofibers. The common peaks at 31.7°, 34.4°, 36.2°, 47.5°, 56.6°, 62.8°, 67.9° and 69.1° correspond to ZnO wurtzite structure crystal planes (100), (002), (101), (102), (110), (103),(200),(112) and (201) respectively. Additional peaks at 32.5° , 35.5° , 38.7° , 46.3° , 48.7° , 53.5° , 58.3° , 61.5° , 65.9° , 66.1° , 68.1° ,69.2° corresponds to ($\bar{1}$00), (002), (111), ($\bar{1}$12), ($\bar{2}$02), (020), (202), ($\bar{1}$13), (022),($\bar{3}$11), (113), ($\bar{2}$20) planes of CuO. Furthermore, the decrease in the intensities of ZnO peaks in Cu doped ZnO can be clearly attributed to the presence of Cu in ZnO (Barreca et al. ,2011).

The preferred position for Figure 2

UV-visible spectroscopy was carried out to study the optical absorbance properties of the pure ZnO nanofibers and Cu doped ZnO nanofibers and is shown in Fig.3A. The room temperature UV-absorption spectrum of the pure ZnO nanofiber shows a prominent exciton band at 377 nm corresponds which matches with absorption spectra of ZnO reported in the literature. In Copper doped ZnO fibers, absorption peak shifted about 47 nm towards the longer wavelength to band at 427 nm. The red shift of the UV absorption spectroscopy is attributed to the narrowing of the band gap (E_g) owing to the formation of ZnO-CuO heterostructure. The first order estimate of the band gap of Cu doped ZnO nanofibers is calculated to be 2.90 eV as compared to the band gap of pure ZnO nanofibers which is 3.28 eV.

Before surface immobilization of antibodies onto Cu-doped nanofibers using chemisorption, it is essential to ensure the presence of functional groups post MPA treatment. For this purpose, FTIR spectroscopy was carried out both on untreated and MPA treated Cu-doped Zinc Oxide nanofibers and is depicted in Fig.4B. In the finger print region of the spectra, the peak seen in the range of 552 - 417 cm^{-1} is due to ZnO stretching in the sample.The broad peaks at 3740 - 3000 cm^{-1} and 1524 - 1691 cm^{-1} is due to O-H stretching and O-H bending respectively. The bands at 1900 - 2354 cm^{-1} are assigned to the CO adsorption on the surface of oxide while the bands at 780 - 980 cm^{-1} assigned to the peroxide formation (M-O-O-M). All other peaks are attributed to the characteristic of the prepared pure and MPA treated CZnO nanofibers (Labhane et al. ,2015). In addition bands near at 1550 cm^{-1} and 1410 cm^{-1} can be attributed to the asymmetric and symmetric stretches vibrations of the carboxylic group of the acid treated nanofiber (Chen et al.,2008; Ojam¨ae et al., 2006).

The preferred position for Figure 3

3.2. Electrochemical Studies

Cyclic voltammetric studies were conducted to investigate the electro chemical behavior of MPA treated CZnO nanofibers(fCZnONFs) in a wide potential range of -0.4 to 0.8 V in presence of 5.0mM $[Fe(CN)6]^{3-/4-)}$]. Fig. 4A shows the cyclic voltagram(CV) obtained for bare GCE, GCE/CZnONF, GCE/fCZnONF/Anti-HRP2 bioelectrode.The peak to peak voltage (ΔE) of bare GCE was found to be 0.1

V while (ΔE) for GCE/CZnONF was estimated to be 0.51V. The larger peak to peak difference indicates slower electron transfer of [[$Fe(CN)_6$] $^{3-/4-}$)] species towards the bioelectrode owing to the presence of ZnO. The insulating character of ZnO nanofiber also resulted in slightly decreased current (50µA) compared to that of bare GCE (103µA). After incorporation of Anti-HRP2 and BSA via covalent interaction post MPA treatment, the magnitude of current is found to decrease because of insulating nature of proteins which acts as a barrier for electron transport.

Electrochemical impedance spectroscopy is one of the best electroanalytical techniques for studying adsorption processes. The key parameter that is monitored in EIS is the charge transfer resistance which critically depends on the composition of the electrode surface. The charge transfer resistance of the standard redox couple [[$Fe(CN)_6$] $^{3-/4-}$)] depends on the tunneling distance between the electrode and the couple. Higher the tunneling distance, higher is the resistance. The electrochemical impedance spectroscopy performed in 0.01M PBS (PH 7.4) solution containing 5 mM [[$Fe(CN)_6$] $^{3-/4-}$)] with the frequencies swept from 0.01 Hz-10 KHz. The impedance behavior of the different % of Cu doped and undoped ZnO nanofiber modified GCE electrodes were conducted (Fig.S2). The charge transfer resistance values were extracted by fitting the data using a standard Randles electrical equivalent circuit (Bard and Faulkner (1980)). The R_{ct} at the GCE/CZnONF is much smaller than that of the GCE/ZnO electrode indicating the improved electrochemical activity after doping with Cu. Doping concentration was optimized to 4% of Cu because of the difficulty in the formation of nanofibers due to electrostatic repulsion and segregation of Cu in the grain boundaries at higher Cu concentrations. The Cu-ZnO nanofiber composite with 4% doping concentration was used for carrying out further experiments. The EIS spectra obtained for various modified electrodes are shown in Fig 4B. The R_{ct} value of GCE/ CZnONF bioelectrode(7.6 kΩ) is found to increase as compared to that of bare GCE electrode (319 Ω). This is attributed to semiconducting/insulating nature of ZnO nanofiber modified on the GCE surface. The MPA treatment of bio electrode generates the functional groups on the CZnONF surface for covalent immobilization of proteins. As expected, after the conjugation of BSA and Anti-HRP2 on the surface of the GCE/fCZnONF bioelectrode, the Rct value was again found to increase (13.5 kΩ). This is due to the loading of proteins (both BSA and Anti-HRP2) molecules, hinders the diffusion of electrons produced in the oxidation/reduction of [$Fe(CN)_6$] $^{3-/4-}$)] ions towards the bioelectrode.

The preferred position for Figure 4

3.3. Electrochemical impedance spectroscopy (EIS) detection of Malaria Histidine- Rich Protein II (HRP2)

The electrochemical response of GCE/fCZnONF/Anti-HRP2 bioelectrode was investigated as a function of HRP2 protein concentration using EIS technique in 0.01M PBS (PH 7.4) solution containing F e$(CN)_6]^{3-/4-}$ over the frequency range from 0.01Hz to 10kHZ using an amplitude of 5 mV. Fig. 5A shows the nyquist plots of EIS experiments carried out as a function of HRP-2 concentration (ag/ml − µg/ml). When antibody functionalized, Cu-doped ZnO nanofiber modified GCE is used as working electrode the corresponding antigen gets immobilized onto the electrode surface through immunoassay reaction. This adsorption increases the tunneling distance and inhibits the electron transfer process thereby increasing the charge transfer resistance. The amount of adsorption which is the proportional to the bulk concentration of the antigen can be correlated to the percentage change in the charge transfer resistance. The detection of ultra-low concentrations is attributed to the presence of CuO/ZnO heterojunction interface which lowers the band gap thereby enhancing electron transfer between electrode-electrolyte in conjunction with high surface area of MPA treated CZnOnFs for protein conjugation. In the case of Cu doped ZnO nanofibers, the surface concentration of antibodies is found to be 11.05% higher as compared to the undoped ZnO nanofibers estimated using Langmuir adsorption isotherm which relates the charge transfer resistances (Rct) of the respective electrodes with surface concentration θ. (Rosales-Rivera et al., 2011). Thus copper doped Zinc oxide nanofiber provides excellent biosensing platform compared to those of other materials.

The theoretical model for the dynamic process of impedance change which occurs through the antigen–antibody coupling is proposed and validated by O.A. Sadik et al (Sadik et al., 2002). From the basic electrical impedance scheme, the equivalent impedance of the redox probe is a parallel combination of electrode impedance, interface impedance and the bulk impedance. The change in interface impedance is a dynamic process and it critically depends on the number of antibodies on the surface and the number of antigens that are getting bound by replacing the solvated electrolyte molecules at a particular time instance. During antigen –Antibody interaction, the impedance, Z_{Ag}, of any newly bound antigen, replaces the impedance, Z_0, of the electrolyte that has previously occupied. For one-to-one binding scheme, the impedance, $Z_{interface}(t)$, of the interface at time t, is given by

$$\frac{1}{Z_{interface}(t)} = \frac{N_{Ag(t)}}{Z_{Ag}} + \frac{N_{AB} - N_{Ag(t)}}{Z_0} \qquad (1)$$

where, $N_{Ab}$is the number of active antibody present at the surface of the working electrode, and $N_{Ag(t)}$denoting the number of antigen bound at time t.

The resulting relation between the impedance changes ΔZ, the ratio of number of bound antigens at a particular time instance t with respect to the number of antibodies on the surface can be expressed as

$$\frac{N_{Ag(t)}}{N_{Ab}} = \frac{1}{(\Delta Z(t)+1)(1-{Z_0}/{Z_{Ag}})} \qquad (2)$$

Where, the impedance change ΔZ is related to the ratio of ${Z_0}/{Z_{Ag}}$. Thus the relative amount of antigen bound can be estimated with respect to the impedance change. However, an absolute value determination might be possible only by knowing the antibody loading at the surface from the prior calibration procedures.

A standard calibration curve for GCE/fCZnONF/Anti-HRP2 bioelectrode is plotted as charge transfer resistance R_{ct} (in linear scale) versus HRP2 concentration (on a logarithmic scale). The Experimental data were fitted to a Rodbard's four parameter logistic function describing a sigmoidal binding curve as shown in Fig. 5B(curve 1) which is followed by Eq. (4) (Warwick,1996). A significant increase in the impedance signal was observed between 10 ag/mL and 10 µg/mL of HRP2 concentration which could potentially differentiate from the blank measurement (curve 2).

$$Y = \frac{-66.03}{1+({x}/{8.92*10^{-18}})^{1/0.08}} + 50.2 \qquad (3),$$

where, Y is the charge transfer resistance R_{ct} corresponding to HRP2 concentration x. The limit of detection (LOD) is calculated as,

$$\text{LOD} = EC_{50}\left(\frac{A_1 - A_2}{A_1 - A_2 - (3\sigma)}\right)^{1/P} \qquad (4),$$

where, A_1 is the minimum asymptote and A_2 is the maximum asymptote, EC_{50} is the concentration corresponding to the 50% of the maximal signal change (inflection point), σ is the Standard Deviation of Blank and P is the slope at the inflection point of the sigmoid curve. The limit of detection (LOD) for GCE/fCZnONF/Anti-HRP2 is low (6.8ag) when compared to those reported in the literature based on malaria detection (Table S1). A significant variation in charge transfer resistance (R_{ct}) is observed in a wide range of HRP2 concentration (10 ag/ml −10 µg/ml) and the relative standard deviation (RSD) of the measurement was in the range of 0.53%-1.3%. The linear part of the sigmoidal fitted curve is plotted as charge transfer resistance R_{ct} versus logarithmic value of the HRP2 concentrations (Fig. 6B(Inset)), and the fabricated GCE/fCZnONF/Anti-HRP2 bioelectrode exhibits a very high sensitivity of about 28.5KΩ/ (g/ml)/cm^2 (with $R^2 = 0.982$).

The preferred position for Figure 5

The stability and reproducibility of the immunosensors is also a key factor in fabrication of biosensor. The stability and reproducibility of GCE/fCZnONF/Anti- HRP2 biosensor was investigated by repeating the detection of 10ag/ml of HRP2 protein after two months. No significant change was observed in the impedance response and it retained 86.5% of the initial value with a relative standard deviation (RSD) value of 2.3 %, clearly indicating that immunosensor exhibits good stability (Fig.S3). The decrease in the impedance response may be due to the denaturation of biomolecules. These biosensors were regenerated at the fixed HRP2 concertation (10pg/ml) after treated with glycine-HCl (0.2M, pH2.5) solution for two minutes. The regeneration efficiency was found to be 96.1% of the initial signal which indicate that the biosensor can be used again. The interference studies were performed using various concentration of interfering agents such as human IgG and BSA along with HRP2 protein detection (Fig.S4). No remarkable difference of impedance response was observed in comparison with the result obtained in the presence of HRP2 alone. This is evident by the low relative standard deviation (RSD = 1.9%), indicating that the selectivity of the biosensor is acceptable.

4. Conclusions

In this paper, we demonstrate the applicability of Cu doped Zinc Oxide Electrospun nanofibers for ultrasensitive detection of malarial parasites. The sensitivity is enhanced by carrying out chemisorption of antibodies onto the nanofibers using Mercaptopropylphosphonic acid (MPA) self-

assembled monolayers. MPA enhances the functional groups required for immobilizing antibody. Cu doping in ZnO not only increases the conductivity of the nanofibers but also preconcentrates the target analyte onto the nanofiber surface due to the resultant of electric field inherently generated at the CuO/ZnO heterojunction interface. The impedimetric detection response of Cu-doped ZnO nanofiber modified electrode shows excellent sensitivity (28.5 KΩ/(g/ml)/cm^2 with a lower detection limit of 6.8 ag/ml. To the best of our knowledge this is the lowest detection limit of malarial parasites reported in the literature. Since the nanobiosensor platform is based on immunoassay technique, with a little modification, it can be extended for developing point-of-care diagnostic devices for several biomarkers of importance.

References

Ahmad, M., Pan, C., Luo, Z., Zhu, J., 2010a. A single zno nanofiber-based highly sensitive amperometric glucose biosensor. The Journal of Physical Chemistry C 114, 9308–9313.

Ahmad, M., Pan, C., Zhu, J., 2010b. Electrochemical determination of cysteine by an elbow shaped, sb-doped zno nanowire-modified electrode.Journal of Materials Chemistry 20, 7169–7174.

Ahmad, R., Tripathy, N., Hahn, Y.B., 2014. Highly sensitive hydrazine chemical sensor based on zno nanorods field-effect transistor. Chemical360 Communications 50, 1890–1893.

Ali, M.A., Mondal, K., Singh, C., Malhotra, B.D., Sharma, A., 2015. Anti-epidermal growth factor receptor conjugated mesoporous zinc oxide nanofibers for breast cancer diagnostics. Nanoscale 7, 7234–7245.

Bard, A.J., Faulkner, L.R., 1980. Electrochemical methods: fundamentals and applications. volume 2. Wiley New York.

Barreca, D., Carraro, G., Comini, E., Gasparotto, A., Maccato, C., Sada, C., Sberveglieri, G., Tondello, E., 2011. Novel synthesis and gas sensing performances of cuo–tio2 nanocomposites functionalized with au nanoparticles.The Journal of Physical Chemistry C 115, 10510–10517.

Batra, N., Tomar, M., Gupta, V., 2015. Zno–cuo composite matrix based reagentless biosensor for detection of total cholesterol. Biosensors and Bioelectronics 67, 263–271.

Bojdi, M.K., Mashhadizadeh, M.H., Behbahani, M., Farahani, A., Davarani, S.S.H. and Bagheri, A., 2014. Synthesis, characterization and application of novel lead imprinted polymer nanoparticles as a high selective electrochemical sensor for ultra-trace determination of lead ions in complex matrixes. *Electrochimica Acta 136* ,59-65.

Bojdi, M.K., Behbahani, M., Sahragard, A., Amin, B.G., Fakhari, A. and Bagheri, A., 2014. A palladium imprinted polymer for highly selective and sensitive electrochemical determination of ultra-trace of palladium ions.Electrochimica Acta *149*, 108-116.

Bojdi, M.K., Behbahani, M., Mashhadizadeh, M.H., Bagheri, A., Davarani, S.S.H. and Farahani, A., 2015. Mercapto-ordered carbohydrate-derived porous carbon electrode as a novel electrochemical sensor for simple and

sensitive ultra-trace detection of omeprazole in biological samples. *Materials Science and Engineering: C 48*, 213-219.

Campuzano-Zuluaga, G., H¨anscheid, T., Grobusch, M.P., 2010. Automated haematology analysis to diagnose malaria. Malaria journal 9, 346.

Chen, Z., Chen, H., Hu, H., Yu, M., Li, F., Zhang, Q., Zhou, Z., Yi,379 T., Huang, C., 2008. Versatile synthesis strategy for carboxylic acid functionalized upconverting nanophosphors as biological labels. Journal of the American Chemical Society 130, 3023–3029.

Chotivanich, K., Silamut, K., Day, N.P., 2006. Laboratory diagnosis of malaria infection. Australian Journal of Medical Science 27, 11.

Chow, L., Lupan, O., Chai, G., Khallaf, H., Ono, L., Cuenya, B.R., Tiginyanu, I., Ursaki, V., Sontea, V., Schulte, A., 2013. Synthesis and characterization of cu-doped zno one-dimensional structures for miniatur-ized sensor applications with faster response. Sensors and Actuators A:388 Physical 189, 399–408.

Dai, Z., Shao, G., Hong, J., Bao, J., Shen, J., 2009. Immobilization and direct electrochemistry of glucose oxidase on a tetragonal pyramid-shaped porous zno nanostructure for a glucose biosensor. Biosensors and Bioelectronics 24, 1286–1291.

Das, M., Sumana, G., Nagarajan, R., Malhotra, B., 2010. Application of nanostructured zno films for electrochemical dna biosensor. Thin Solid Films 519, 1196–1201.

Demirev, P.A., 2004. Mass spectrometry for malaria diagnosis .Doolan, D.L., Mu, Y., Unal, B., Sundaresh, S., Hirst, S., Valdez, C., Randall,A., Molina, D., Liang, X., Freilich, D.A., 2008. Profiling humoral immune responses to p. falciparum infection with protein microarrays. Proteomics 8, 4680.

Erdman, C., Emerson, J.W., 2008. A fast bayesian change point analysis for the segmentation of microarray data. Bioinformatics 24, 2143–2148.

Fontecha, G.A., Mendoza, M., Banegas, E., Poorak, M., De Oliveira, A.M., Mancero, T., Udhayakumar, V., Lucchi, N.W., Mejia, R.E., 2012. Comparison of molecular tests for the diagnosis of malaria in honduras. Malaria journal 11, 119.

Gikunoo, E., Abera, A., Woldesenbet, E., 2014. A novel carbon nanofibers grown on glass microballoons immunosensor: A tool for early diagnosis of malaria. Sensors 14, 14686–14699.

Gong, H., Hu, J., Wang, J., Ong, C., Zhu, F., 2006. Nano-crystalline cu doped zno thin film gas sensor for co. Sensors and Actuators B: Chemical 115, 247–251.

Hong, H., Shi, J., Yang, Y., Zhang, Y., Engle, J.W., Nickles, R.J., Wang, X., Cai, W., 2011. Cancer-targeted optical imaging with fluorescent zinc oxide nanowires. Nano letters 11, 3744–3750.

Hosseini, H., Behbahani, M., Mahyari, M., Kazerooni, H., Bagheri, A. and Shaabani, A., 2014. Ordered carbohydrate-derived porous carbons immobilized gold nanoparticles as a new electrode material for electrocatalytical oxidation and determination of nicotinamide adenine dinucleotide. Biosensors and Bioelectronics 59, 412-417.

Johnston, S.P., Pieniazek, N.J., Xayavong, M.V., Slemenda, S.B., Wilkins,P.P., da Silva, A.J., 2006. Pcr as a confirmatory technique for laboratory diagnosis of malaria. Journal of clinical microbiology 44, 1087–1089.

Kalate Bojdi, M., Behbahani, M., Najafi, M., Bagheri, A., Omidi, F. and Salimi, S., 2015. Selective and Sensitive Determination of Uranyl Ions in Complex Matrices by Ion Imprinted Polymers-Based Electrochemical Sensor.Electroanalysis *27*, 2458-2467.

Kifude, C.M., Rajasekariah, H.G., Sullivan, D.J., Stewart, V.A., Angov,E., Martin, S.K., Diggs, C.L., Waitumbi, J.N., 2008. Enzyme-linked immunosorbent assay for detection of plasmodium falciparum histidine-rich protein 2 in blood, plasma, and serum. Clinical and vaccine immunology 423 15, 1012–1018.

Labhane, P., Huse, V., Patle, L., Chaudhari, A., Sonawane, G., 2015. Synthesis of cu doped zno nanoparticles: Crystallographic, optical, ftir, morphological and photocatalytic study. Journal of Materials Science and Chemical Engineering 3, 39.

Lillehoj, p.B., Huang, M.C., Truong, N., Ho, C.M., 2013. Rapid electrochemical detection on a mobile phone. Lab on a chip 13, 2950—2955.

Mali, S.S., Kim, H., Jang, W.Y., Park, H.S., Patil, P.S., Hong, C.K., 2013.Novel synthesis and characterization of mesoporous zno nanofibers by electrospinning technique. ACS Sustainable Chemistry & Engineering 1, 1207–1213.

Moody, A., 2002. Rapid diagnostic tests for malaria parasites. Clinical microbiology reviews 15, 66–78.

Ojam¨ae, L., Aulin, C., Pedersen, H., K¨all, P.O., 2006. Ir and quantumchemical studies of carboxylic acid and glycine adsorption on rutile tio2 nanoparticles. Journal of colloid and interface science 296, 71–78.

Poon, L.L., Wong, B.W., Ma, E.H., Chan, K.H., Chow, L.M., Abeyewickreme, W., Tangpukdee, N., Yuen, K.Y., Guan, Y., Looareesuwan, S.,2006a. Sensitive and inexpensive molecular test for falciparum malaria:detecting plasmodium falciparum dna directly from heat-treated blood by loop-mediated isothermal amplification. Clinical chemistry 52, 303–306.

Poon, L.L., Wong, B.W., Ma, E.H., Chan, K.H., Chow, L.M., Abeyewickreme, W., Tangpukdee, N., Yuen, K.Y., Guan, Y., Looareesuwan, S.,2006b. Sensitive and inexpensive molecular test for falciparum malaria:detecting plasmodium falciparum dna directly from heat-treated blood byloop-mediated isothermal amplification. Clinical chemistry 52, 303–306.

Rakotonirina, H., Barnadas, C., Raherijafy, R., Andrianantenaina, H., Ratsimbasoa, A., Randrianasolo, L., Jahevitra, M., Andriantsoanirina, V.,M´enard, D., 2008. Accuracy and reliability of malaria diagnostic techniques for guiding febrile outpatient treatment in malaria-endemic countries. The American journal of tropical medicine and hygiene 78, 217–221.

Rosales-Rivera, L. C., Acero-Sánchez, J. L., Lozano-Sanchez, P., Katakis, I., & O'Sullivan, C. K., 2011. Electrochemical immunosensor detection of antigliadin antibodies from real human serum. Biosensors and Bioelectronics 26, 4471-4476.

Sadik, O. A., Xu, H., Gheorghiu, E., Andreescu, D., Balut, C., Gheorghiu, M., & Bratu, D.,2002. Differential impedance spectroscopy for monitoring protein immobilization and antibody-antigen reactions. *Analytical chemistry 74*,3142-3150

Shapiro, H.M., Mandy, F., 2007. Cytometry in malaria: moving beyond giemsa. Cytometry Part A 71, 643–645.Sharma, M.K., Rao, V.K., Agarwal, G.S., Rai, G.P., Gopalan, N., Prakash,S., Sharma, S., Vijayaraghavan, R., 2008. Highly sensitive amperometricimmunosensor for detection of plasmodium falciparum histidine-rich protein 2 in serum of humans with malaria: comparison with a commercial kit. Journal of clinical microbiology 46, 3759–3765.

Sikarwar, B., Sharma, P.K., Srivastava, A., Agarwal, G.S., Boopathi, M.,Singh, B., Jaiswal, Y.K., 2014. Surface plasmon resonance characterization of monoclonal and polyclonal antibodies of malaria for biosensor.Biosensors and Bioelectronics 60, 201–209.

Sim˘s´ıkov´a, M., Antal´ık, M., Ka˘nuchov´a, M., ˘ Skvarla, J., 2013. Anionic 11- ˘ mercaptoundecanoic acid capped zno nanoparticles. Applied Surface Sci-ence 282, 342–347.

Singhal, S., Kaur, J., Namgyal, T., Sharma, R., 2012. Cu-doped zno nanoparticles: Synthesis, structural and electrical properties. Physica B: Condensed Matter 407, 1223–1226.

Snow, R.W., Guerra, C.A., Noor, A.M., Myint, H.Y., Hay, S.I., 2005. The global distribution of clinical episodes of plasmodium falciparum malaria.Nature 434, 214–217.

Solanki, P.R., Kaushik, A., Agrawal, V.V., Malhotra, B.D., 2011. Nanostructured metal oxide-based biosensors. NPG Asia Materials 3, 17–24.

Sonawane, Y.S., Kanade, K., Kale, B., Aiyer, R., 2008. Electrical and gassensing properties of self-aligned copper-doped zinc oxide nanoparticles.Materials Research Bulletin 43, 2719–2726.

de Souza Castilho, M., Laube, T., Yamanaka, H., Alegret, S., Pividori, M.,2011. Magneto immunoassays for plasmodium falciparum histidine-rich protein 2 related to malaria based on magnetic nanoparticles. Analytical chemistry 83, 5570–5577.

Tak, M., Gupta, V., Tomar, M., 2013. Zinc oxide–multiwalled carbon nanotubes hybrid nanocomposite based urea biosensor. Journal of Materials Chemistry B 1, 6392–6401.

Tak, M., Gupta, V., Tomar, M., 2014. Flower-like zno nanostructure based electrochemical dna biosensor for bacterial meningitis detection. Biosensors and Bioelectronics 59, 200–207.

Vasudev, A., Kaushik, A., Bhansali, S., 2013. Electrochemical immunosensor for label free epidermal growth factor receptor (egfr) detection. Biosensors and Bioelectronics 39, 300–305.

Warhurst, D., Williams, J., 1996. Acp broadsheet no 148. july 1996. laboratory diagnosis of malaria. Journal of Clinical Pathology 49, 533.

Warwick, M.J., 1996. Cap 8. Standardisation of immunoassay. In: Brian,L. (Ed.), Immunoassay, A Practical Guide. Taylor & Francis Ltd.,London, UK, p. 160.

Wei, Y., Li, Y., Liu, X., Xian, Y., Shi, G., Jin, L., 2010. Zno nanorods/auhybrid nanocomposites for glucose biosensor. Biosensors and Bioelectronics 496 26, 275–278.
Wongchotigul, V., Suwanna, N., Krudsood, S., Chindanond, D., Kano, S.,Hanaoka, N., Akai, Y., Maekawa, Y., Nakayama, S., Kojima, S., 2004.The use of flow cytometry as a diagnostic test for malaria parasites. The Southeast Asian Journal of Tropical Medicine and Public Health 35, 552–559.

Yatsushiro, S., Yamamura, S., Yamaguchi, Y., Shinohara, Y., Tamiya, E.,Horii, T., Baba, Y., Kataoka, M., 2010. Rapid and highly sensitive detection of malaria-infected erythrocytes using a cell microarray chip. PloSone 5.

Zhang, Z., Li, X., Wang, C., Wei, L., Liu, Y., Shao, C., 2009. Zno hollow nanofibers: fabrication from facile single capillary electrospinning and applications in gas sensors. The Journal of Physical Chemistry C 113,19397–19403.

Zhao, Z., Chen, X., Tay, B., Chen, J., Han, Z., Khor, K., 2007. A novel amperometric biosensor based on zno: Co nanoclusters for biosensing glucose.Biosensors and bioelectronics 23, 135–139.

Figures and Captions

Figure 1: (A) FESEM images of (a) ZnO nanofibers berofore calcination (b) after calcination (c) Cu doped ZnO nanofiber before calcination (d) and after calcination. (B) EDX spectra of electrospun Cu doped ZnO nanofibers with quantitative composition.

Figure 2: XRD analysis of the ZnO nanofibers (blue curve) and Cu doped ZnO nanofibers (red curve).

Figure 3: (A) UV-VIS absorption spectra of ZnO nanofiber (blue curve) and Cu doped ZnO nanofiber (red curve).(B) FTIR spectra of Cu doped ZnO nanofiber (red curve) MPA treated Cu doped ZnO nanofiber (blue curve).

Figure 4: (A) Cyclic voltammetry (CV) studies of various fabricated bioelectrodes at a scan rate of 50 mVs^{-1} and (B) Electrochemical impedance spectroscopy (EIS) studies of various fabricated bioelectrodes.

Figure 5: (A) Impedance response of the GCE/fCuZnONFs/Anti-HRP2 bioelectrode as a function of HRP2 concentration. (B) Calibration curve of the biosensor using a logarithmic scale fitted to sigmoidal curve (curve 1).The fabricated biosensor could potentially differentiate the impedance signal observed between 10 ag/mL and 10 µg/mL of HRP2 concentration which lies above the blank measurement (curve 2) and inset shows the dynamic linear range.

Figure 1

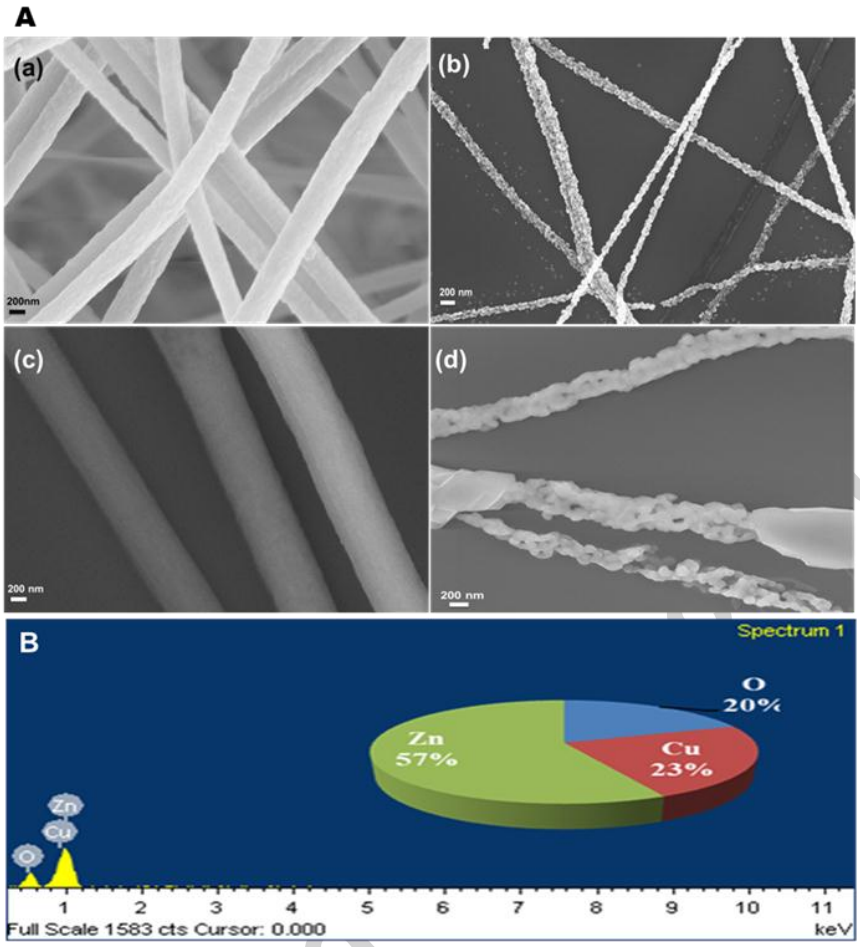
A
(a)
200nm
(b)
200 nm
(c)
200 nm
(d)
200 nm
B
Spectrum 1
O
20%
Zn
57%
Cu
23%
Zn
Cu
O
1
2
3
4
5
6
7
8
9
10
11
Full Scale 1583 cts Cursor: 0.000
keV

Figure 2

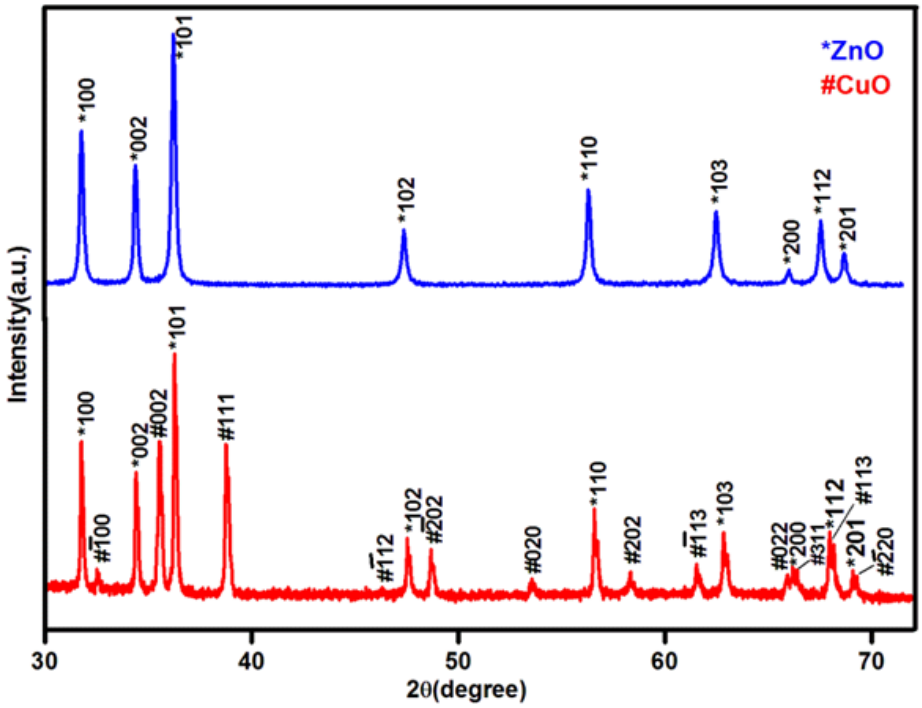
*ZnO
#CuO
Intensity(a.u.)
2θ(degree)
30
40
50
60
70
*100
*002
*101
*102
*110
*103
*200
*112
*201
#100
#002
#111
#112
#202
#020
#202
#113
#022
#200
#311
#220

Figure 3

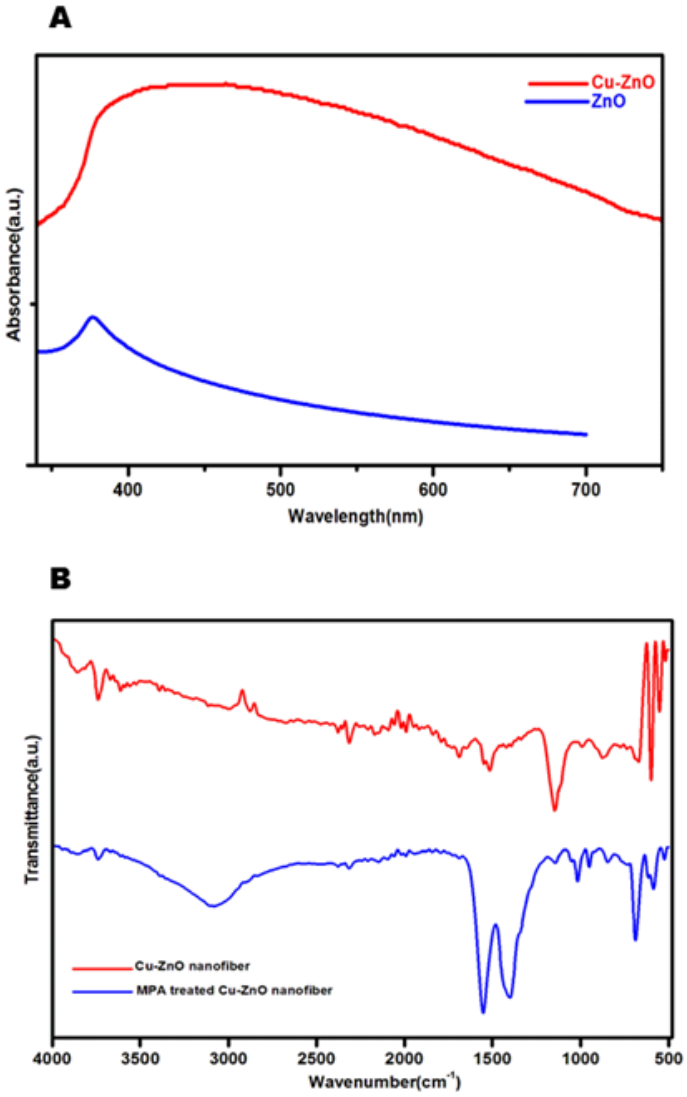

Figure 4

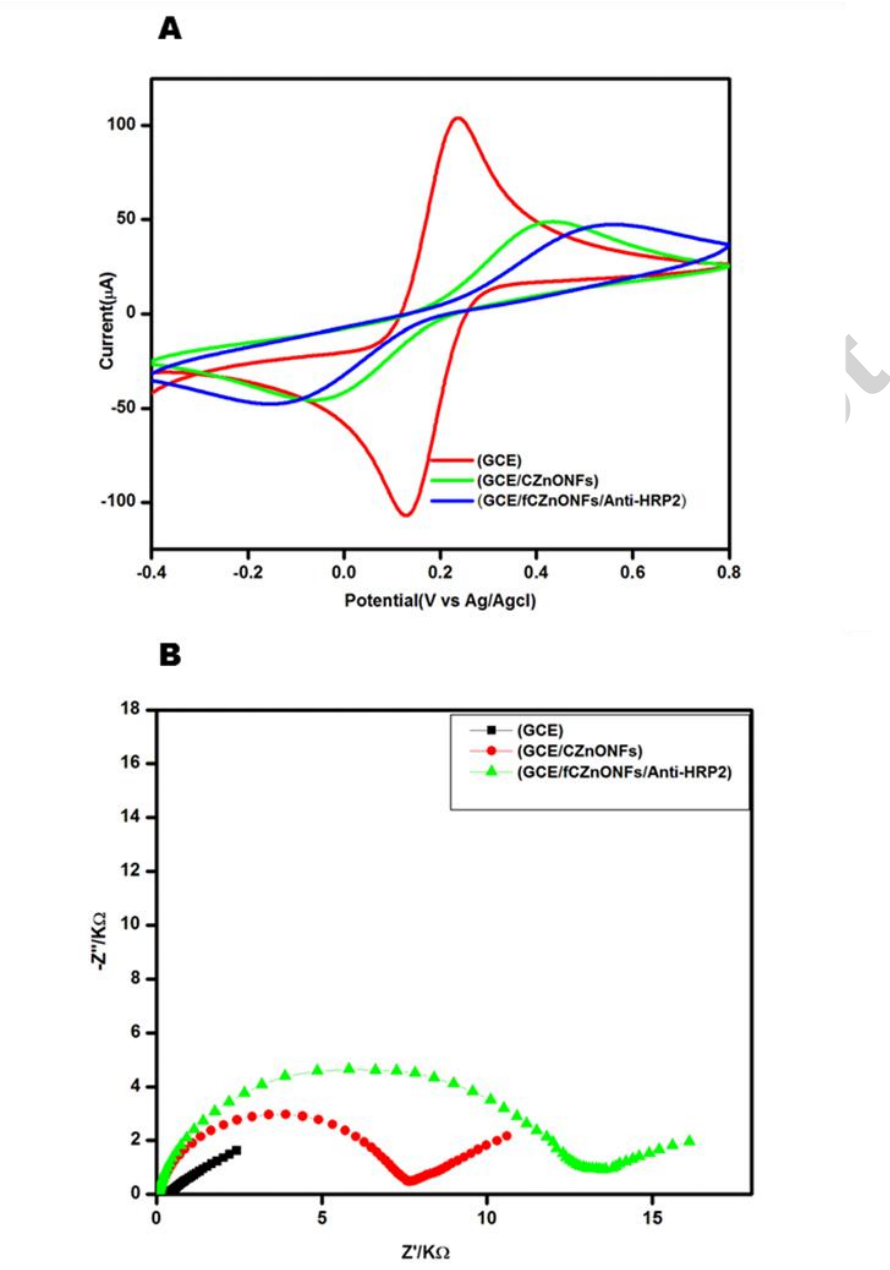

Figure 5

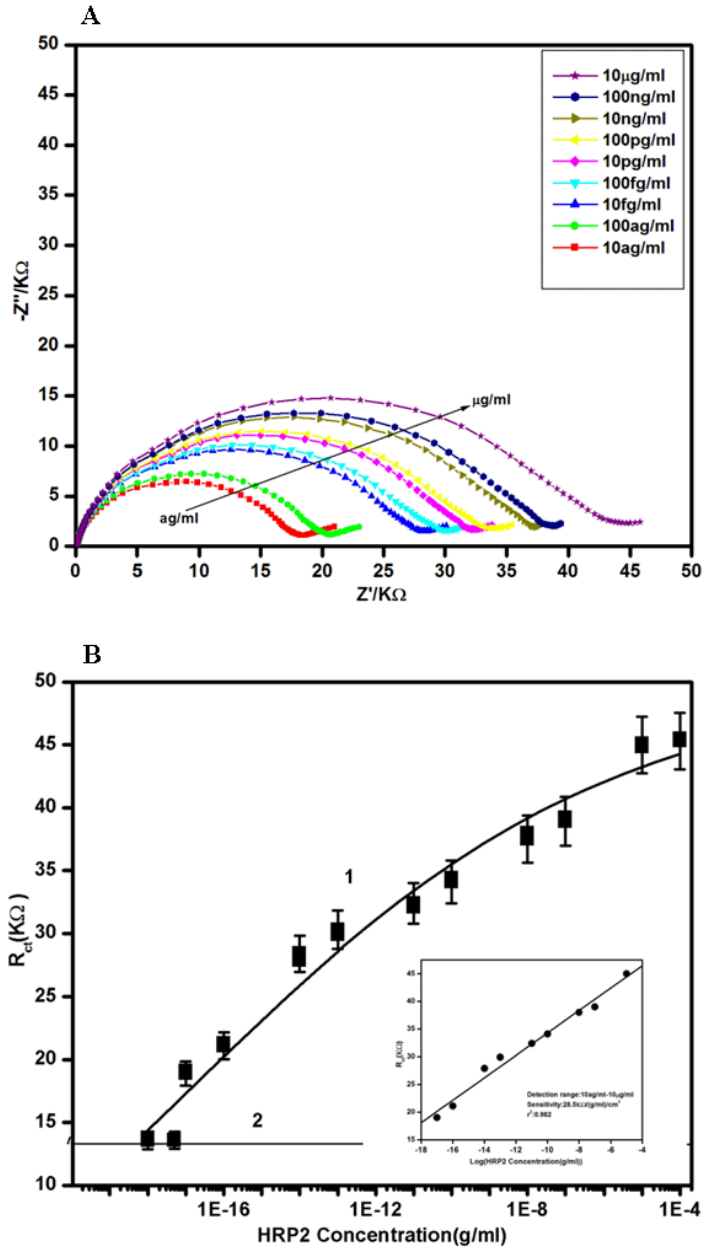
A
10μg/ml
100ng/ml
10ng/ml
100pg/ml
10pg/ml
100fg/ml
10fg/ml
100ag/ml
10ag/ml
μg/ml
ag/ml
-Z''/KΩ
Z'/KΩ
B
1
2
R_{ct}(KΩ)
HRP2 Concentration(g/ml)
1E-16
1E-12
1E-8
1E-4

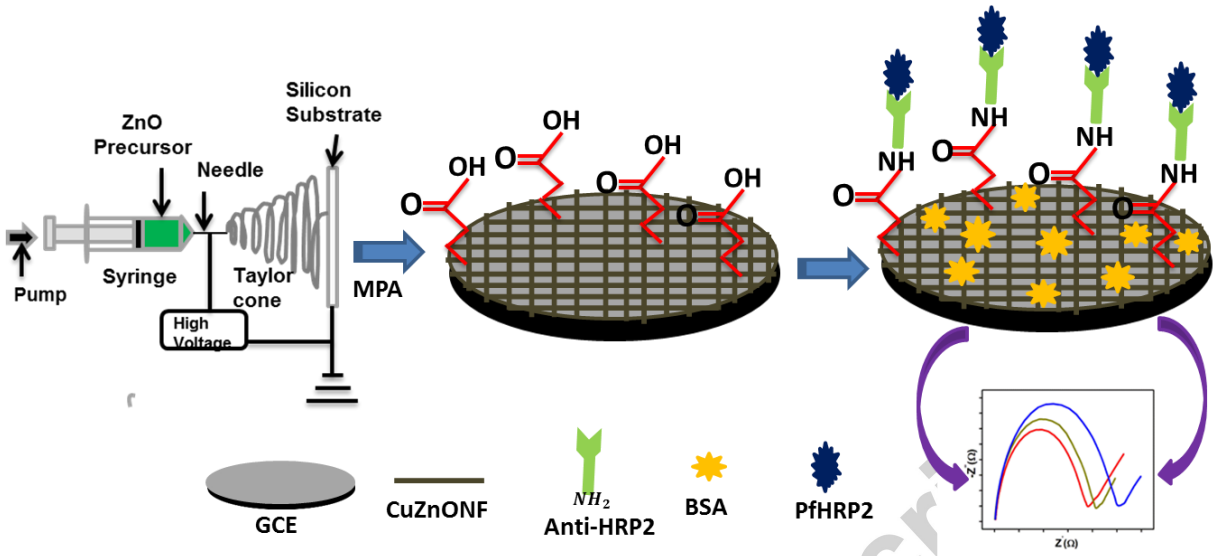

Highlights

- **Cu doping in ZnO nanofiber: Breakthrough in attogram/ml malaria parasite detection**
- **Simple and low cost method of doping by electrospinning**
- **A novel surface modification for generating functional groups**
- **A novel platform for developing point-of-care diagnostic devices**